



Controlled formation of shape structures via electrochemical surface modification of Cu(111)

Vicente Pascual-Llorens^{a,b}, Albert Serrà-Ramos^{c,d}, Paula Sebastián-Pascual^{a,*}

^a Wallenberg Initiative Materials Science for Sustainability, Department of Chemistry, School of Engineering Science in Chemistry, Biochemistry and Health, KTH Royal Institute of Technology, Stockholm, Sweden

^b Center for High Entropy Alloy Catalysis, Department of Chemistry, University of Copenhagen, Universitetsparken 5, 2100 Copenhagen, Denmark

^c Grup d'Electrodeposició de Capes Primes i Nanoestructures (GE-CPN), Departament de Ciència de Materials i Química Física, Universitat de Barcelona, Martí i Franquès, 1, 08028 Barcelona, Catalonia, Spain

^d Institute of Nanoscience and Nanotechnology (IN2UB), Universitat de Barcelona, 08028 Barcelona, Catalonia, Spain

ARTICLE INFO

Keywords:

Copper single facet
Chloride
High-index facets
Shape tetrahedral clusters
Square-wave potential method

ABSTRACT

Electrochemical oxidation-reduction processes on copper electrodes and in the presence of different electrolyte anions have been widely explored for the preparation of tailor-made catalysts. Nevertheless, the effect of the electrode surface structure and electrolyte on the growth of new crystalline domains on copper remains under discussion. In this work, we have modified a Cu(111) single crystalline electrode with chloride by using the square-wave potential method, aiming to reach a higher control on the formation of shape structures. In particular, we have modified the single-facet surface by applying potential pulses with a frequency of 1 Hz and between -1.3 V and 0.5 V vs SCE. Then, we evaluated the formation of new structures with scanning electron microscopy after different times of applied potential pulses. The morphology analysis revealed the formation of hexagonal micro and nanoclusters homogeneously distributed on the surface. These clusters were similar to tetrahedral particles embedded in the (111) plane. Moreover, we also observed a shape transformation from a hexagonal particle to a triangular pyramid, showing that crystal growth and evolution are time and structure dependent. Herein, we provide experimental insights on the preparation of (n10) micro and nanostructures of copper using the square-wave potential method. The present work offers a straightforward approach that enables precise control over the rational preparation of copper surfaces.

1. Introduction

Copper-based materials have earned considerable interest due to their unique properties that make them suitable for several electrocatalytic reactions such as the carbon dioxide (CO₂) reduction [1], the conversion of biomass-derived aldehydes [2,3] or the nitrate reduction [4]. Nevertheless, the composition and geometry of the active surface sites on copper significantly influence the efficiency and product selectivity of these reactions [5–7]. Consequently, a significant number of studies have been conducted to investigate different strategies to prepare tailor-made surfaces, with the aim of improving the catalytic performance of copper-based materials [8].

One common strategy to tune the surface structure of copper is the application of electrochemical oxidation–reduction processes in the presence of different electrolyte anions [9–12]. Typically, during the

oxidation–reduction process, copper is firstly oxidized and dissolved, and then redeposited again in the form of metallic copper, a copper oxide or a copper salt. The deposited structures display different morphology depending on the type of anion present in the solution. Under reductive conditions, the oxide or copper salt phase is further converted into metallic copper [12–14]. In the past years, numerous studies have reported the impact of chloride anions on the modification of copper polycrystalline surfaces via oxidation–reduction processes. These studies observed the formation of copper chloride and oxide nanocubes which usually became rugous under electrochemical reductive conditions [15–18]. Some of these studies suggested that chloride also induced the generation of sites with (100) geometry [19,20], site geometry that is considered favourable for electrochemical CO₂ reduction. [21] Alternatively, it was also proposed that the electrochemical oxidation-reduction process significantly increased the number of low

* Corresponding author.

E-mail address: paulasp@kth.se (P. Sebastián-Pascual).

<https://doi.org/10.1016/j.electacta.2025.145793>

Received 29 October 2024; Received in revised form 28 January 2025; Accepted 2 February 2025

Available online 3 February 2025

0013-4686/© 2025 The Author(s). Published by Elsevier Ltd. This is an open access article under the CC BY license (<http://creativecommons.org/licenses/by/4.0/>).

coordinated sites, active sites for catalysis, or induced surface roughening [12,22,23]. However, the identity and distribution of sites geometries formed when the copper electrode is oxidized and reduced remains under discussion, underscoring the necessity to find electrochemical methods to precisely tune and characterize the surface structure.

In our previous works, we evaluated the effect of chloride anions on the electrochemical reconstruction of a polycrystalline copper electrode by applying triangular potential cycles at fast scan rates between 200 and 500 mV s^{-1} [24,25]. With this method we obtained tetragonal stepped pyramids in some electrode areas. The analysis of the lead underpotential deposition (Pb UPD) cyclic voltammograms (CVs) of the modified surfaces and density functional theory (DFT) calculations suggested that chloride induced the formation of (n10) domains, i.e., surfaces with (100) terraces and (110) steps. We concluded that the growth of the observed tetragonal shape structures was linked to the formation of (n10) domains. [24]. To tune the facet distribution on copper, we applied potential cycles between a reduction potential limit (E_R) -1.0 V and an oxidation potential limit (E_o) that varied between 0.5 and 2.0 V vs SCE, observing the formation of a higher number of new sites by increasing the applied oxidation potential limit. Nevertheless, our studies also showed that the morphology of the modified polycrystalline surface was highly dependent on the substrate quality [25]. Polycrystalline electrodes have multiple grains, grain boundaries and irregularities which can reconstruct in different ways because oxidation–reduction processes are structure sensitive [26,27]. Although we illustrated the formation of shape tetragonal pyramids covering large electrode areas, we also found other zones that became highly irregular, rough and presented signs of corrosion [25]. We ascribed those results to the fact that those electrode zones were more active resulting in the development of a rugos morphology when they were modified via potential cycling. Thus, the assessment of anion effects on the reconstruction of a polycrystalline electrode is complex because polycrystalline surfaces have numerous grains and defects which exhibit different crystal nucleation and growth mechanisms [28].

To rationally address the effect of the substrate orientation on the formation of a new crystalline structure, in this work we have carried out the modification of a well-defined copper single crystalline electrode. A single facet is a preferentially oriented flat surface that ideally contains only one or two site geometries, allowing for the investigation of substrate effects on electrochemical oxidation–reduction processes [29]. For this study, we have modified a Cu(111) single facet because its voltammetric behaviour has been broadly investigated in many model studies in electrochemistry and electrocatalysis [30–33]. In this instance, the Cu(111) single facet surface was modified by using the square-wave potential (SWP) method rather than by applying potential cycles. This potential pulse technique has been previously used to induce changes in the copper surface structure in a controlled way [12,19,34]. Prior to the works on surface modification of copper, A. J. Arvia and co-workers [27] first used the SWP method to electrochemically induce surface re-faceting on a platinum polycrystalline electrode. Later, S.G. Sun and co-workers demonstrated that control preparation of shape structures of Pd and Pt with high-index facets could be achieved with the SWP method by controlling parameters such as potential-pulse frequency and potential limit conditions [35–37].

In this work, we have applied potential pulses between -1.3 V (E_R) and 0.5 V vs SCE (E_o), with a frequency of 1 Hz between pulses, to modify the Cu(111) electrode in a 0.1 M NaCl solution. We apply -1.3 V vs SCE as the reduction limit because at this potential value the hydrogen evolution reaction does not occur or it is negligible in the NaCl electrolyte, but copper is fully reduced and electrodeposited. The oxidation limit was maintained at the low potential value of 0.5 V, at which no oxygen evolution reaction takes place, but there is dissolution of Cu to Cu^{2+} [38]. With these potential limits we aim to perform the surface modification of copper at a high deposition rate [37] but with decreased etching rate, to control the electrode dissolution and

re-growth process and reduce surface roughening [34]. Ultimately, we aim to assess the effect of applying potential pulses on the crystal growth of copper at different stages or deposition times. We perform the electrochemical surface modification in a solution of 0.1 M NaCl, as we did in our previous reports [24,25], to ensure that chloride adsorption/desorption on copper is driving the nucleation and growth processes of the new crystal structures.

Then, to address the change in surface structure we have recorded Pb UPD CVs of the modified Cu(111) surfaces at different times. Metal UPD involves the deposition of a sub monolayer of metal atoms onto a foreign metallic surface at potentials prior to the bulk potential deposition. The potential difference between a monolayer and the bulk potential deposition of the deposited metal varies with the orientation of the surface electrode because different surface geometries have different work functions [39]. Moreover, the anion adsorption, which competes with the metal UPD process, is also facet dependent [40]. Consequently, the metal UPD display voltammetric features which shape and potential value highly depends on the number and structure of the surface sites. Thus, it allows calculating the electroactive surface area and determine crystallographic domains of different geometry [24,25]. In this work, we combine cyclic voltammetry technique and scanning electron microscopy (SEM) to gain insight into the effect of chloride, substrate orientation and deposition time on the formation of copper shape structures prepared with the SWP method.

2. Experimental

All electrochemical experiments were carried out in a classical three-electrode cell configuration, using a glass cell with four entries and a lugging capillary for the reference electrode. The reference electrode was a saturated calomel electrode (SCE). The working electrode was a Cu(111) with 99.999 % purity and purchased from Mateck company. All experiments were conducted with the working electrode maintained in the hanging meniscus configuration under an argon atmosphere. Prior to each experiment, the working electrode surface was electropolished in a two-electrode cell containing a diluted solution of 70 % phosphoric acid (prepared from phosphoric acid 85 %, VMR Chemicals, Prolabo®). Subsequently, a constant potential difference (ΔE) of 2.0 V was applied between the Cu(111) (anode) and a copper wire (cathode) for 30 seconds (s). Finally, the electropolished surface was rinsed with ultrapure water to remove the excess of acid, after which it was transferred to the electrochemical cell. All the electrochemical experiments were conducted using a VSP-300 biologic multipotentiostat (BioLogic). Before the experiments, the glassware and the glass cells were kept overnight in a saturated solution of KMnO_4 (Sigma Aldrich, Emplura®), which was employed to oxidize all organic pollutants. Thereupon, the glassware was rinsed with a diluted solution of H_2O_2 (33 %, VMR Chemicals, Prolabo®) + H_2SO_4 (96 %, Sigma Aldrich, Suprapur®) with ultrapure water, to remove the MnO_2 waste, and was boiled three times in ultrapure water.

The CVs of the Pb UPD on the reconstructed Cu(111) as well as on different Cu single facets were performed at pH 3. The electrolyte solution consisted of 0.1 M of KClO_4 (99.95 %, Sigma-Aldrich Merck) + 2 mM of NaCl (99.9 % Sigma-Aldrich Merck) + 2 mM of $\text{Pb}(\text{ClO}_4)_2 \cdot \text{H}_2\text{O}$ (99.995 %, Sigma-Aldrich Merck) + 1 mM HClO_4 (70 %, Sigma Aldrich Merck, Suprapur®). The CVs were performed between -0.4 V and -0.2 V vs SCE at a scan rate of 5 mV s^{-1} . Alternatively, we have also performed an additional voltammetric analysis of the different copper surfaces by recording the blank CVs in 0.1 M NaCl at a scan rate of 50 mV s^{-1} , between -1.2 V and -0.3 V vs SCE. To modify the Cu(111) electrode, potential pulses between -1.3 V and 0.5 V vs SCE with a frequency of 1 Hz were applied for different times between 45 s and 3600 s and in 0.1 M NaCl.

The Scanning Electron Microscopy (SEM) analysis was performed before and after the Pb UPD to confirm the presence of metallic copper and that the Pb UPD does not modify the copper surface morphology.

Then, the modified Cu(111) was cleaned with abundant ultrapure water. The morphology of the chloride-modified electrode was analysed using a JEOL 7800 F prime SEM from the University of Copenhagen at low voltage (4 keV) and FESEM JEOL J-7100 SEM from the University of Barcelona. Energy Dispersive Spectroscopy (EDS) was carried out alongside the SEM characterization to further confirm the absence of chloride or other contaminants on the modified electrode.

We have used VESTA (Visualization for Electronic and Structural Analysis) software to draw the crystalline and atomic structures of cubic and tetrahedral (n10) particles.

3. Results

3.1. Surface modification of Cu(111) at different times

Prior to the examination of the modification of the Cu(111) electrode with chloride, we have evaluated its surface ordering by recording the Pb UPD CVs after electropolishing it. We electropolish the Cu(111) surface before each new experiment in order to remove the modification induced by chloride. Fig. S1 illustrates the evolution of the Pb UPD CVs of the Cu(111) subjected to multiple electropolishing cycles for months. The CV displays a single, intense cathodic peak at -0.31 V vs SCE, with a counter peak appearing at -0.28 V vs SCE in the anodic region. The different Pb UPD CVs only show slight alterations in their profile, and the integrated charge remains nearly unchanged. The peak at -0.31 V vs SCE becomes slightly broader after the continued performance of a greater number of experiments. The obtained CV profiles for a Cu(111) are similar to those we reported previously [24,25] and the CVs reported

by Brisard et al. [41], suggesting that the surface maintains its preferential (111) orientation, but there is a relatively small increase of the amount of defects overtime. Fig. S2 shows the SEM images of the Cu(111) surface, at different magnifications, which does not have any feature or grain boundary as in a polycrystalline substrate (Fig. S2D), suggesting that it is a relatively flat surface.

After the examination of the Cu(111) surface condition, we addressed the reconstruction of Cu(111) in 0.1 M NaCl solution. The modification was achieved by applying potential-pulse programs at three different deposition time ranges named as: short deposition times (between 45 and 150 s), moderate times (between 300 and 600 s) and long deposition times (between 1800 and 3600 s). We started applying short potential-pulse programs of 45 and 150 s. Fig. 1A depicts the Pb UPD CV of the Cu(111) surface treated for 150 s. The reduction sweep of the Pb UPD CV exhibits three main decoupled peaks at -0.31 V (P1), -0.32 V (P2) and -0.35 V (P3) vs SCE. In contrast, the non-symmetric counter peaks show a major overlapping in the anodic region [24]. A direct comparison of this CV with that of Cu(111) and other single facets reported in our previous studies [24,25], suggests that P1 corresponds to (111) sites, P2 may contain low coordinated sites, such as (110) sites and defects [25], whereas P3 is close to the (310) single facet peak.

Fig. 1B depicts the SEM images of the modified Cu(111) at 150 s, which demonstrate the formation of a high population of copper microstructures with a hexagonal pyramidal shape. These shape clusters are distributed homogeneously on the surface, covering areas exceeding $100 \mu\text{m}$ (Fig. S3). The hexagonal clusters have different sizes, suggesting that the redeposition of copper with potential pulses exhibits a progressive behaviour [42,43]. Some of these structures are less symmetric

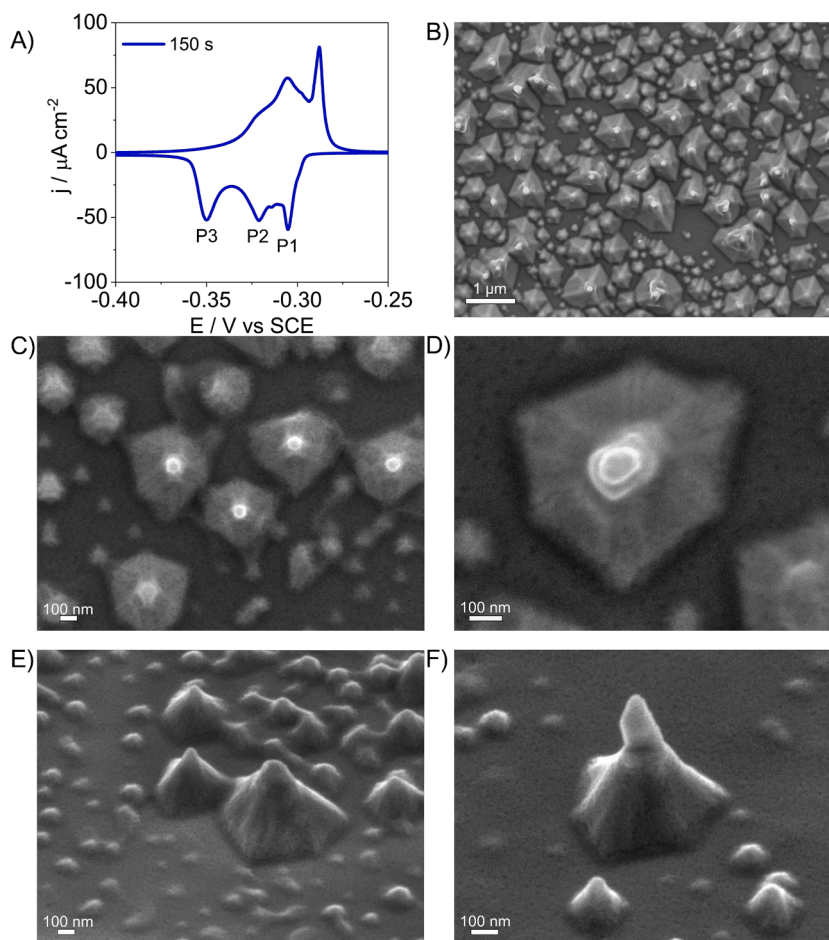


Fig. 1. A) Pb UPD CV of a Cu(111) surface modified with chloride for 150 s; SEM images of the Cu(111) modified for different times: B) 150 s, C)-F) 45 s. E) and F) were recorded at an angle of 45° between the electron beam and the line normal to the surface plane.

than others, which could be due to differences in the nucleation, growth and dissolution processes at atomic sites located at the edges and corners of the new structures, or at substrate defects [27,44]. Fig. 1C and D illustrates SEM images of the Cu(111) surface modified at 45 s, captured at higher magnifications to elucidate the initial stages of micro and nanostructure formation. At 45 s, the formation of nanoclusters with a hexagonal shape is already visible, with size range between 100 and 500 nm. Notably, these nanoclusters show an intense bright spot at the apex of the hexagonal structure, where the six-sides converge. To better address these bright spots, an analysis of the surface morphology was conducted at an angle of 45° between the SEM beam and the surface normal, aiming to examine the morphology features from a different perspective. Figs. 1E and S4 illustrate a conglomerate of these structures at varying growth stages, showcasing the hexagonal pyramidal shape induced by the chloride anion as well as the formation of tips at the apex of the biggest structures. Fig. 1F contains a zoomed image of a hexagonal cluster with a prominent tip, which is likely the origin of the shiny zones in the SEM of Fig. 3D. This result shows that the growth of copper tends to be faster at the apex of the hexagonal clusters. The formation of tips at the apex of the clusters could be related to an electric field effect on the copper redeposition process. Previous articles addressing electric field effects on the CO₂ reduction on gold needles reported that the local electric field is higher at the corners and tips of catalyst surfaces, areas which are rich in low coordinated sites [45]. The higher local electric field in these zones contributed to stabilize the CO₂ intermediates via attraction of electrolyte cations, thus increasing the activity for the CO₂ reduction. Similarly, we suggest that the formation of copper tip structures is possibly caused by the higher local electric field at the apex of the shape structures that attract more Cu²⁺ ions, resulting in higher deposition rates.

In order to more accurately assess the impact of chloride on the reconstruction mechanism of Cu(111), we applied a series of potential-pulse programs at moderate times between 300 and 600 s. Fig. 2 depicts the Pb UPD CV of the Cu(111) surface that was treated for 300 s, along with the corresponding SEM images. Fig. 2A illustrates three main peaks in the cathodic sweep, analogous to those observed in the Pb UPD in Fig. 1A. The (n10) peak (P3) has significantly increased in intensity, whereas the intensity of the other two peaks increases to a lesser extent. Fig. 2B displays a higher surface coverage and the formation of large hexagonal microstructures with sharp edges, as observed under SEM analysis. These larger symmetric structures appear to be surrounded by multiple smaller shape structures, which highlights the progressive nature of the oxidation–reduction process mechanism. These shape structures are also significantly stepped [24].

To shed lights into the results from Figs. 2A–C, we have added simulated shape particles with variable (111), (310) and (100) facet ratios in Fig. 2D. We have assumed that chloride induces (n10) sites with short terrace domains such as (210) (2x(100)x(110)) or (310) (3x(100)x(100)) sites [24]. Particles I–III in Fig. 3D follows the transition process from octahedral shape with (111) facets to tetrahedral shape with (310) sides. A hexagonal pyramid with six (310) sides emerges along the (111) direction, as seen in (III), a shape that is similar to the shape of the microstructures in the recorded SEM image in Fig. 2B. This similitude between deposited and simulated particles points out that the orientation of the substrate determines the growth direction of the new crystals, leading to the formation of tetrahedral clusters embedded in the (111) plane. The formation of steps in the sides of the hexagonal structures also suggests a tendency of the new crystallographic phase to expand along the (100) direction (Figs. 2B–C and DIII)). Remarkably, the microscale edges of the steps in Fig. 2C grow following a pattern similar to the distribution of atomic steps on a (n10) particle deposited on a (111) plane, as shown in Fig. 2DIV). As illustrated in Fig. S5, extending the duration of the potential-pulse program to 600 s causes the formation of larger microstructures. Fig. S5A illustrates the Pb UPD of the modified Cu(111), which has a similar profile to that one obtained at 300 s, with a slightly more intense (n10) peak. The SEM images in

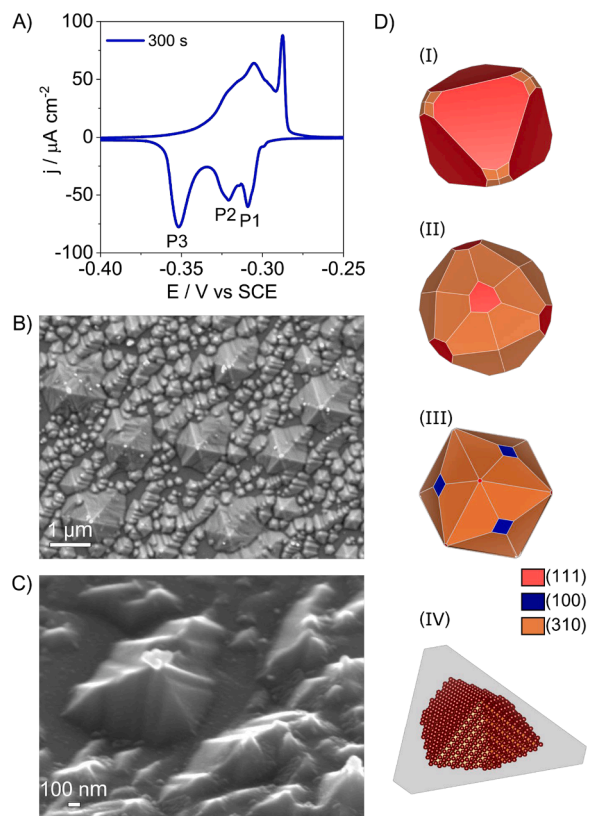


Fig. 2. A) Pb UPD CV on Cu(111) surface, which has been modified for 300 s; B) and C) SEM images of the modified Cu(111) surface for 300 s. C) was recorded at an angle of 45° between the electron beam and the surface normal; D) simulated shape particles morphologies with varied (111), (100), and (310) facets.

Figs. S5B and S5C show larger structures, all of them being more similar in size than the obtained at shorter deposition times of 150–300 s. Figs. S5B and S5C also show that at 600 s, the microstructures begin to overlap and change shape.

To gain further insight into structure aspects of the reconstructed surface, we performed extended experiments for >600 s. Fig. 3A depicts the Pb UPD CV of the Cu(111) surface modified for 1800 s. As expected, the (n10) peak has increased in intensity, while other peaks at lower potential values (P1 and P2) have undergone a less significant change. Figs. 3B and 3C contain the SEM images of the modified Cu(111) at 1800 s, which shows the formation of structures of variable shape and big clusters of several micrometres. The formation of these structures results in an increase of the electroactive surface area or roughness factor (RF) of 1.5 with respect to the bare Cu(111) surface. To calculate the RF of the chloride-modified Cu(111) surfaces we integrated the charge involved in the cathodic region of the voltammetric Pb UPD curves. We have included in the supporting information the details for the determination of the RF of each Cu surface. Table S1 contains the calculated RF values for the modified Cu(111) at different times, which shows a progressive increase in active area from ca. 1.15 at 150 s to 1.52 at 1800 s. Like the deposits at 300 s and 600 s (Figs. 2C and S5), Fig. 3C also shows a significant amount of stepped features emerging from the laterals of the deposited clusters at 1800 s. Notably, most of the deposited structures have lost the characteristic hexagonal shape, and only the smallest particles formed at the earlier stages of the oxidation–reduction process retain this shape. Surprisingly, a few new structures with a tendency to develop a triangular pyramidal shape have emerged. We have highlighted some of these structures with a red circle in Fig. 3C and D. These results suggest a change in the reconstruction mechanism at longer deposition times, with a shape transformation from a hexagonal

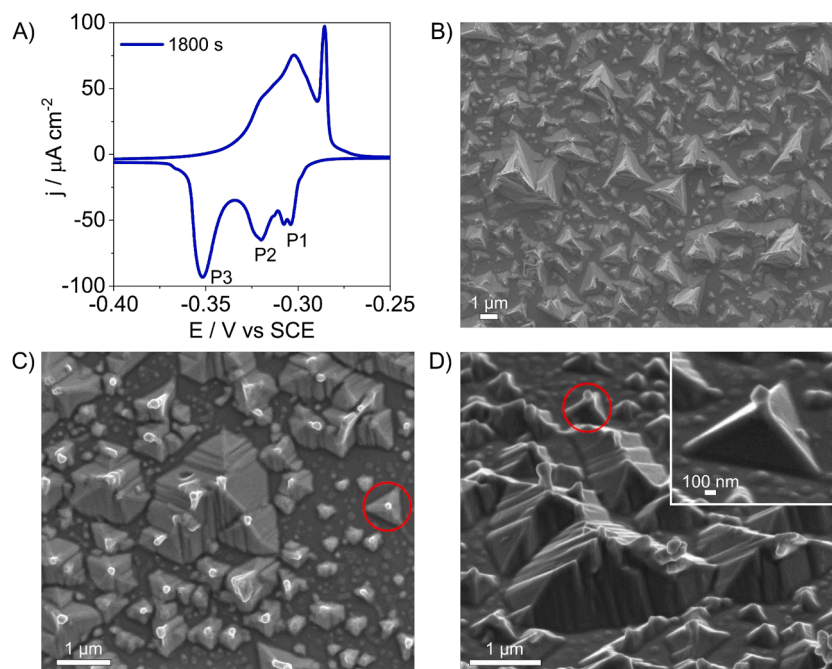


Fig. 3. A) Pb UPD CV on Cu(111) surface, which has been modified for 1800 s; B), C), and D) SEM images of the modified Cu(111) surfaces for 1800 s. D) was recorded at an angle of 45° between the electron beam and the surface normal.

pyramid to a more triangular pyramid structure. The inset in Fig. 3D is a high magnification of one of these triangular pyramids, which also presents a tip or excess of copper deposit at the apex of the clusters. Fig. S6 shows a different area of the electrode modified for 1800 s which bright spots correspond to uncontrolled growth of copper tips on top of the apex of the clusters. As abovementioned, we hypothesize that the formation of copper tips could be related to the higher local electric field at the apex region of the deposited clusters [45].

Finally, we have performed the surface modification of Cu(111) for 3600 s. Fig. 4A shows the Pb UPD CV of the modified surface, which peak P3 is clearly the most intense voltammetric feature. Extending the duration of the potential pulse program to 3600 s leads to the formation of copper clusters of several microns homogeneously distributed on the surface, with a tendency to adopt a more triangular shape as seen in Fig. 5B. At higher magnifications, the SEM illustrates the presence of big structures of several microns with several edges and a high degree of coalescence.

3.2. Analysis of surface structures

To get more insights on which specific (n10) structures are formed by chloride, we carried out an analysis of the conjunction of angles between the sides of several tetrahedral clusters deposited at 45 s. The measurement of the angles to evaluate the crystal facets of shape particles have been previously done for different metal particles such as Pt [37] or CuAu [46]. In this analysis, we have chosen examples of clusters deposited at 45 s, nearly at the early stages of formation of several nanoscale shape structures. Then, we compared the angles of the experimental samples with the conjunction of angles between the six facets of several theoretical (n10) tetrahedral structures placed along a (111) plane. This configuration best represents the growth of (n10) clusters on a (111) surface. n represents the number of atomic rows in the (100) terraces of the $n(100) \times (110)$ structures.

Fig. S7 shows three images of three different isolated shape nano-clusters. Then we have drawn a perimeter around the clusters and calculated the angles between the six sides, obtaining two groups of three angles for each sample: Sample 1 shows angles between 102° and 110°, and between 133° and 137°; 102°–103° and 135°–140° for sample

2; and 106°–115° and 126°–133° for sample 3. On the left side of Fig. S7 we depicted three model (n10) structures with $n = 2, 3$ and 4, respectively, and inserted a (111) grey plane crossing the particle. The angles between the six sides in a (210) cluster are the same: 120°. For a (310) cluster, we have two groups of 98° and 142°. For a (410) cluster, these groups of angles are 88° and 152°. This analysis would support that chloride tends to form structures containing (210) and (310) sites, i.e. with short (100) terrace domains and (110) steps at the very early stages of the modification process. At longer deposition times, there is a shape evolution, which results in the formation of a few triangular pyramids on the surface. To explain the appearance of various shapes at different times, we have depicted in Fig. S8 (n10) nanoparticles with $n = 3, 5$ and ∞ . More cubic particles with longer (100) terraces tend to develop a triangular shape when they grow in the direction perpendicular to a (111) plane. Thus, we hypothesize that chloride favours the formation of (n10) domains with short (100) terrace domains at the early stages of the oxidation-reduction process, with a slightly higher presence of (100) sites over time. This result would be in line with several previous articles [12,19,20] that claimed that chloride induces (100) sites on copper and low coordinates sites, such as (110) steps.

In order to get more insights about which sites are present on the copper surface after prolonged deposition times, we have performed a double voltammetric analysis depicted in Fig. 5. In Fig. 5A, we have plotted the Pb UPD CVs of the (111), (110), (100) and (310) single facets together with the Pb UPD of a Cu(111) surface modified for 600 s. On the other side, in Fig. 5B we have plotted the blank CVs of the single facets in 0.1 M NaCl. We recorded the blank CVs in the potential region between the solvent reduction and the onset of copper oxidation and dissolution. This window corresponds to the potential range between -1.2 V and -0.3 V vs SCE in 0.1 M NaCl, in which only capacitive and interfacial processes take place. Then we have performed the oxidation-reduction modification of a Cu(111) in the same electrolyte between -1.3 V and 0.5 V vs SCE for 600 s and have plotted the resultant blank CV together with the blank CVs of the unmodified single facets. We have chosen 0.1 M NaCl as electrolyte to record the base CVs because chloride is an anion that specifically adsorbs on copper, providing sharp and distinct voltammetric features for each facet orientation [47].

The Pb UPD analysis in Fig. 5A shows that the most intense peak (P3

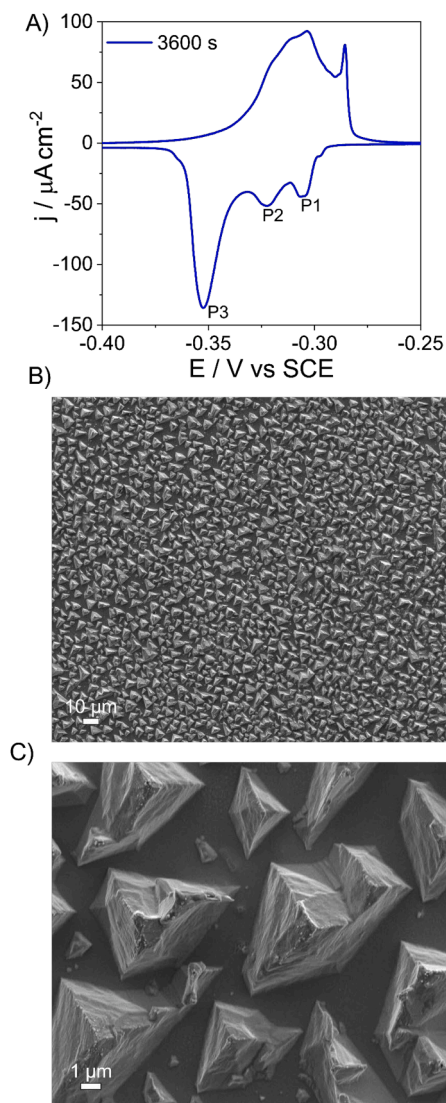


Fig. 4. A) Pb UPD CV of a Cu(111) surface modified with chloride for 3600 s; B) and C) are SEM images of the modified Cu(111) at different magnifications.

at -0.35 V) is closer to the (310) facet (orange dashed line). However, P3 is slightly broad and shows a tiny shoulder or current around -0.36 V vs SCE which corresponds to the position of the (100) facet in the Pb UPD (purple dashed line). The result suggests the presence of (n10) and some (100) sites but since the peak separation between the (310) and the (100) in Pb UPD is small (ca. 10 mV), it is difficult to identify (n10) stepped domains with different terrace length (n). Alternatively, the blank CVs in 0.1M NaCl provide peaks for each facet that are considerably more separated in the potential window, although they are much less intense than the Pb UPD peaks. The blank CV of the modified Cu (111) for 600 s (blue line) contains multiple features. Interestingly, the most pronounced peak x_3 at -0.78 V vs SCE almost aligns with the sharp peak of the (310) facet, and the small x_4 peak (-0.83 vs SCE) and broader one (x_6 at -1.06) aligns with the features of the (100) facet. x_1 and x_2 could be related to (110) and defects, respectively, whereas the remaining x_5 peak coincides with the (111) facet. The good alignment between these two different voltammetric techniques suggests the presence of a mixture of (n10) and some (100) terrace sites on the modified Cu(111).

The origin of the shape transition over time, with the formation of a few triangular pyramids after long periods of time remains unclear. At the initial stages of the deposition process, most of the substrate

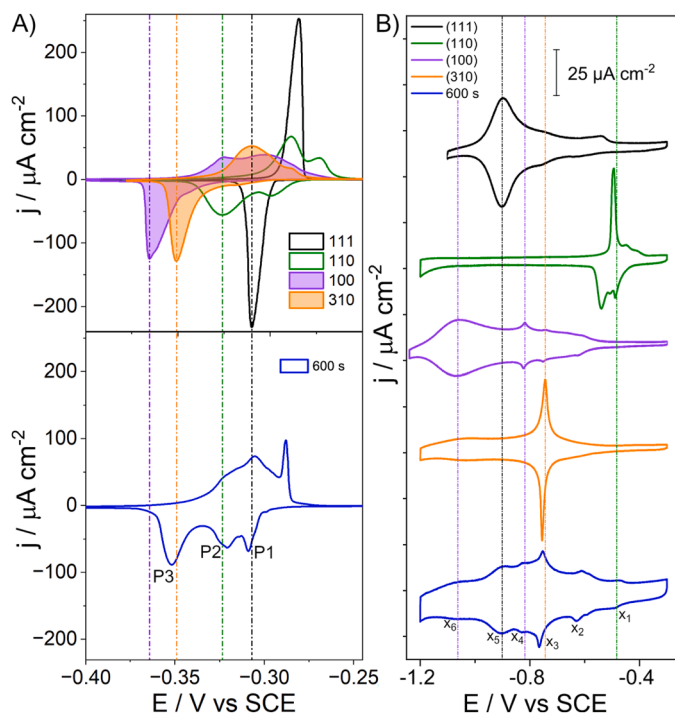


Fig. 5. A) Pb UPD CVs of (111), (110), (100) and (310) facets and the modified Cu(111) for 600 s, recorded at 5 mV s^{-1} . B) Blank CVs in 0.1 M NaCl for the same surfaces at 50 mV s^{-1} .

orientation is (111) leading to the formation of similar structures with tetrahedral shape as seen in Figs. 1 and 2. Here we apply potential limits for high-rate deposition process (-1.3 V vs SCE) and low etching rate (0.5 V vs SCE). Under these conditions we expected the formation of (310) structures driven by chloride adsorption-desorption processes, because chloride stabilize the surface energy of (n10) facets more than other facets, as DFT calculations suggested in our previous work [24]. However, we hypothesize that the accumulation of (n10) sites over time may alter the oxidation-reduction modification mechanism causing a morphology transformation [48]. To partially test this hypothesis, we show in Fig. S9 the modification of the copper polycrystalline electrode from Fig. S2D for 300 s. The SEM in Fig. S9 shows the modification of different grains with well-marked boundaries. It illustrates that the growth direction of the highly stepped structures is different for each grain, as each grain may correspond to a different orientation. Interestingly, while some grains were highly modified, one of them remains slightly changed. This result suggests that copper sites of different geometry may have different rate transformations or stability toward the same oxidation-reduction process in chloride electrolytes. Finding the exact orientation of each grain in a copper polycrystalline electrode with hundreds of them is not possible with the methods presented in this work. However, it is worth mentioning that a recent work by Wahab et al. [49] elaborated a map of surface orientations and activities of different grains in a copper polycrystalline surface using scanning electrochemical microscopy (SECM). We believe that studies with SECM on poly-oriented copper surfaces would serve to address the dynamics of electrochemically induced shape transformations of multiple copper domains in polycrystalline surfaces.

One last aspect to discuss is the progressive formation of hexagonal shape structures of variable size with potential pulses of 1 Hz. Herein we have chosen 1 Hz of frequency because previous works used similar frequencies to induce controlled changes on the surface of a Cu single facet [34] or copper oxide cubes [50]. Remarkably, studies carried out by Arvia [27] and Sun [37] to prepare platinum well defined surfaces with potential pulses used higher frequencies over 10 Hz and up to several kHz. Arvia and co-workers [27] proposed that applying fast

pulses with increased frequency reduced the diffusion layer thickness to values below the irregularities of the surface, reducing the surface roughening. Thus, future works should explore the modification of copper at very high frequency values over 100 Hz and address its effect in the size and shape of the newly formed particles.

Overall, our work shows that the SWP method allows for direct and controlled electrochemical tuning of a Cu(111) surface with tetrahedral clusters embedded on the single facet. As far as we know, electrochemically induced tetrahedral shape particles were reported for Pt and Pd by Sun and co-workers [35,36]. Therefore, we believe that this work opens new opportunities to explore different electrolytes to prepare high-index facet copper surfaces by using the SWP method. High-index facets contain a high density of low coordinated step sites, having interesting catalytic properties for different reactions such as the CO₂ reduction. Recent reports by Roldan-Cuenya and co-workers have demonstrated that flat (111) and (100) surfaces are inactive towards the CO₂ reduction and therefore the presence of steps is critical to obtain an increased performance [33,51].

We also demonstrate that although chloride tends to form (210) and (310) sites on copper at the early stages, the surface modification is sensitive to the substrate orientation and time dependent, leading to a shape transformation overtime. Here we have also presented two different voltammetric analysis, one with Pb UPD and one in NaCl, to evaluate different copper single facets as well as the structure of the modified Cu(111). This double analysis shows that the cyclic voltammetry method provides a unique voltammetric fingerprint of each electrode-electrolyte interface, being an easy but powerful method to obtain structure information of the prepared catalysts.

4. Conclusions

In this study, we have investigated in detail the effect of chloride on the surface modification of Cu(111) using the SWP method, aiming to assess how surface structure and electrolyte anion affect the formation of new sites on copper. The modification of a well-oriented copper crystal facet allowed high control of the deposition process, resulting in the formation of homogeneously distributed shape micro and nanostructures. At the early stages of the process, we deposited clusters with the shape of tetrahedral particles placed along the (111) plane with geometry between (210) and (310) facets. After 30 minutes of applying potential pulses, the hexagonal clusters underwent a transformation and some of them started to develop a more triangular shape, possibly containing a mixture of (100) and (110) sites. Herein, we provide evidence that the electrochemical surface modification of copper is not only dependent on the electrolyte anion or on the potential limits. The substrate structure or orientation, the deposition time and the use of potential pulses rather than potential cycles significantly impact the surface morphology. As such precise control of these parameters is critical for rationally tuning copper surfaces via electrochemical oxidation–reduction processes.

CRediT authorship contribution statement

Vicente Pascual-Llorens: Writing – original draft, Visualization, Validation, Methodology, Investigation, Formal analysis, Data curation. **Albert Serrà-Ramos:** Writing – review & editing, Resources, Methodology, Investigation, Formal analysis, Data curation. **Paula Sebastián-Pascual:** Writing – original draft, Supervision, Resources, Project administration, Methodology, Funding acquisition, Formal analysis, Conceptualization.

Declaration of competing interest

The authors declare the following financial interests/personal relationships which may be considered as potential competing interests:

Paula Sebastian Pascual reports financial support was provided by

Knut and Alice Wallenberg Foundation. Paula Sebastian Pascual reports financial support was provided by Villum Foundation. There are no conflicts of interest. If there are other authors, they declare that they have no known competing financial interests or personal relationships that could have appeared to influence the work reported in this paper.

Acknowledgments

We gratefully acknowledge the Villum Foundation for financially supporting this research through a Villum Young Investigator Grant (project number: 53090). We also thank the Wallenberg Initiative Materials Science for Sustainability (WISE) funded by the Knut and Alice Wallenberg Foundation for financial support. We acknowledge the Department of Chemistry of the University of Copenhagen and the “Servicios Científico Técnicos” of the University of Barcelona for providing facilities to perform this project. A special thanks goes to Prof Elvira Gómez from University of Barcelona for her valuable discussions and guidance in this project. We also thank the members of the group of Surface Electrochemistry at the University of Alicante for valuable discussions.

Supplementary materials

Supplementary material associated with this article can be found, in the online version, at [doi:10.1016/j.electacta.2025.145793](https://doi.org/10.1016/j.electacta.2025.145793).

Appendices

Supplementary information contains CVs of Pb UPD of Cu(111) modified at 600 s and 3600 s and SEM images of the same electrode modified at 45 s, 150 s, 600 s and 3600 s. We have also included experimental details and description of sample preparation and modification.

Data availability

Data will be made available on request.

References

- [1] S.A. Nitopi, E. Bertheussen, S.B. Scott, X. Liu, K. Albert, S. Horch, B. Seger, I.E. L. Stephens, K. Chan, J.K. Nørskov, T.F. Jaramillo, I. Chorkendorff, Progress and perspectives of electrochemical CO₂ reduction on copper in aqueous electrolyte, *Chem. Rev.* 119 (2019) 7610–7672, <https://doi.org/10.1021/acs.chemrev.8b00705>.
- [2] P. Nilges, U. Schröder, Electrochemistry for biofuel generation: production of furans by electrocatalytic hydrogenation of furfurals, *Energy Environ. Sci.* 6 (2013) 2925–2931, <https://doi.org/10.1039/C3EE41857J>.
- [3] T. Wang, L. Tao, X. Zhu, C. Chen, W. Chen, S. Du, Y. Zhou, B. Zhou, D. Wang, C. Xie, P. Long, W. Li, Y. Wang, R. Chen, Y. Zou, X.-Z. Fu, Y. Li, X. Duan, S. Wang, Combined anodic and cathodic hydrogen production from aldehyde oxidation and hydrogen evolution reaction, *Nat. Catal.* 5 (2022) 66–73, <https://doi.org/10.1038/s41929-021-00721-y>.
- [4] M. Duca, M.T.M. Koper, Powering denitrification: the perspectives of electrocatalytic nitrate reduction, *Energy Environ. Sci.* 5 (2012) 9726–9742, <https://doi.org/10.1039/C2EE23062C>.
- [5] E. Pérez-Gallent, M.C. Figueiredo, I. Katsounaros, M.T.M. Koper, Electrocatalytic reduction of nitrate on copper single crystals in acidic and alkaline solutions, *Electrochim. Acta* 227 (2017) 77–84, <https://doi.org/10.1016/j.electacta.2016.12.147>.
- [6] J. Li, N. Kornienko, Probing electrosynthetic reactions with furfural on copper surfaces, *Chem. Commun.* 57 (2021) 5127–5130, <https://doi.org/10.1039/D1CC01429C>.
- [7] A. Bagger, L. Arnarson, M.H. Hansen, E. Spohr, J. Rossmeisl, Electrochemical CO reduction: a property of the Electrochemical interface, *J. Am. Chem. Soc.* 141 (2019) 1506–1514, <https://doi.org/10.1021/jacs.8b08839>.
- [8] H. Mistry, A.S. Varela, S. Kühn, P. Strasser, B.R. Cuenya, Nanostructured electrocatalysts with tunable activity and selectivity, *Nat. Rev. Mater.* 1 (2016) 16009, <https://doi.org/10.1038/natrevmats.2016.9>.
- [9] J. Han, C. Long, J. Zhang, K. Hou, Y. Yuan, D. Wang, X. Zhang, X. Qiu, Y. Zhu, Y. Zhang, Z. Yang, S. Yan, Z. Tang, A reconstructed porous copper surface promotes selectivity and efficiency toward C₂ products by electrocatalytic CO₂ reduction, *Chem. Sci.* 11 (2020) 10698–10704, <https://doi.org/10.1039/D0SC01202E>.

- [10] H. Yano, T. Tanaka, M. Nakayama, K. Ogura, Selective electrochemical reduction of CO₂ to ethylene at a three-phase interface on copper(I) halide-confined Cu-mesh electrodes in acidic solutions of potassium halides, *J. Electroanal. Chem.* 565 (2004) 287–293, <https://doi.org/10.1016/j.jelechem.2003.10.021>.
- [11] J.J. Masana, B. Peng, Z. Shuai, M. Qiu, Y. Yu, Influence of halide ions on the electrochemical reduction of carbon dioxide over a copper surface, *J. Mater. Chem.* 10 (2022) 1086–1104, <https://doi.org/10.1039/D1TA09125E>.
- [12] D. Gao, I. Sinev, F. Scholten, R.M. Arán-Ais, N.J. Divins, K. Kvashnina, J. Timoshenko, B.Roldan Cuenya, Selective CO₂ electroreduction to ethylene and multicarbon alcohols via electrolyte-driven nanostructuring, *Angewandte Chemie - Int. Ed.* 58 (2019) 17047–17053, <https://doi.org/10.1002/anie.201910155>.
- [13] T. Kim, G.T.R. Palmore, A scalable method for preparing Cu electrocatalysts that convert CO₂ into C₂⁺ products, *Nat. Commun.* 11 (2020) 3622, <https://doi.org/10.1038/s41467-020-16998-9>.
- [14] S.J. Raaijman, N. Arulmozhi, M.T.M. Koper, Morphological stability of copper surfaces under reducing conditions, *ACS. Appl. Mater. Interfaces.* 13 (2021) 48730–48744, <https://doi.org/10.1021/acsmi.1c13989>.
- [15] Y. Lum, B. Yue, P. Lobaccaro, A.T. Bell, J.W. Ager, Optimizing C–C coupling on oxide-derived copper catalysts for electrochemical CO₂ reduction, *J. Phys. Chem. C* 121 (2017) 14191–14203, <https://doi.org/10.1021/acs.jpcc.7b03673>.
- [16] F.S. Roberts, K.P. Kuhl, A. Nilsson, High selectivity for ethylene from carbon dioxide reduction over copper nanocube electrocatalysts, *Angewandte Chemie Int. Ed.* 54 (2015) 5179–5182, <https://doi.org/10.1002/anie.201412214>.
- [17] M.G. Kibria, C.-T. Dinh, A. Seifitokaldani, P. De Luna, T. Burdyny, R. Quintero-Bermudez, M.B. Ross, O.S. Bushuyev, F.P. García de Arquer, P. Yang, D. Sinton, E. H. Sargent, A surface reconstruction route to high productivity and selectivity in CO₂ electroreduction toward C₂⁺ hydrocarbons, *Adv. Mater.* 30 (2018) 1804867, <https://doi.org/10.1002/adma.201804867>.
- [18] Y. Kwon, Y. Lum, E.L. Clark, J.W. Ager, A.T. Bell, CO₂ Electroreduction with enhanced ethylene and ethanol selectivity by nanostructuring polycrystalline copper, *ChemElectroChem.* 3 (2016) 1012–1019, <https://doi.org/10.1002/celec.201600068>.
- [19] F.S. Roberts, K.P. Kuhl, A. Nilsson, High selectivity for ethylene from carbon dioxide reduction over copper nanocube electrocatalysts, *Angewandte Chemie.* 127 (2015) 5268–5271, <https://doi.org/10.1002/ange.201412214>.
- [20] C.S. Chen, A.D. Handoko, J.H. Wan, L. Ma, D. Ren, B.S. Yeo, Stable and selective electrochemical reduction of carbon dioxide to ethylene on copper mesocrystals, *Catal. Sci. Technol.* 5 (2015) 161–168, <https://doi.org/10.1039/C4CY00906A>.
- [21] E. Pérez-Gallent, M.C. Figueiredo, F. Calle-Vallejo, M.T.M. Koper, Spectroscopic observation of a hydrogenated CO dimer intermediate during CO reduction on Cu(100) electrodes, *Angewandte Chem. Int. Ed.* 56 (2017) 3621–3624, <https://doi.org/10.1002/anie.201700580>.
- [22] D. Gao, F. Scholten, B.Roldan Cuenya, Improved CO₂ electroreduction performance on plasma-activated Cu catalysts via electrolyte design: halide effect, *ACS. Catal.* 7 (2017) 5112–5120, <https://doi.org/10.1021/acscatal.7b01416>.
- [23] K. Jiang, Y. Huang, G. Zeng, F.M. Toma, W.A. Goddard, A.T. Bell, Effects of surface roughness on the electrochemical reduction of CO₂ over Cu, *ACS. Energy Lett.* 5 (2020) 1206–1214, <https://doi.org/10.1021/acsenergylett.0c00482>.
- [24] P.M. Couce, T.K. Madsen, E. Plaza-Mayoral, H.H. Kristoffersen, I. Chorkendorff, K. N. Dalby, W. van der Stam, J. Rossmeisl, M. Escudero-Escribano, P. Sebastián-Pascual, Tailoring the facet distribution on copper with chloride, *Chem. Sci.* 15 (2024) 1714–1725, <https://doi.org/10.1039/D3SC05988J>.
- [25] V. Pascual-Llorens, A. Serra, P. Mazaira-Couce, M. Escudero-Escribano, P. Sebastián-Pascual, Surface nanostructuring of copper using fluoride and chloride, *ChemElectroChem.* (2024), <https://doi.org/10.1002/celec.202400414>.
- [26] A.V. Rudnev, E.B. Molodkina, M.R. Ehrenburg, R.G. Fedorov, A.I. Danilov, Yu. M. Polukarov, J.M. Feliu, Methodical aspects of studying the electroreduction of nitrate on modified single crystal Pt(hkl) + Cu electrodes, *Russian J. Electrochem.* 45 (2009) 1052, <https://doi.org/10.1134/S1023193509090110>.
- [27] A.J. Arvia, J.C. Canullo, E. Custidiano, C.L. Perdriel, W.E. Triaca, Electrochemical faceting of metal electrodes, *Electrochim. Acta* 31 (1986) 1359–1368, [https://doi.org/10.1016/0013-4686\(86\)87046-3](https://doi.org/10.1016/0013-4686(86)87046-3).
- [28] S. Asperti, R. Hendrikx, Y. Gonzalez-Garcia, R. Kortlever, Benchmarking the electrochemical CO₂ reduction on polycrystalline copper foils: the importance of microstructure versus applied potential, *ChemCatChem.* 14 (2022) e202200540, <https://doi.org/10.1002/cctc.202200540>.
- [29] A. Kolodziej, P. Rodriguez, A. Cuesta, Chapter 4: single-crystal surfaces as model electrocatalysts for CO₂ reduction, in: *RSC Energy and Environment Series*, 2018, pp. 88–110, <https://doi.org/10.1039/9781782623809-00088>.
- [30] A. Tiwari, T. Maagaard, I. Chorkendorff, S. Horch, Effect of dissolved glassware on the structure-sensitive part of the Cu(111) voltammogram in KOH, *ACS. Energy Lett.* 4 (2019) 1645–1649, <https://doi.org/10.1021/acsenergylett.9b01064>.
- [31] P. Sebastián-Pascual, F.J. Sarabia, V. Climent, J.M. Feliu, M. Escudero-Escribano, Elucidating the structure of the Cu-alkaline electrochemical interface with the laser-induced jump temperature method, *J. Phys. Chem. C* 124 (2020) 23253–23259, <https://doi.org/10.1021/acs.jpcc.0c07821>.
- [32] A. Auer, F.J. Sarabia, D. Winkler, C. Griesser, V. Climent, J.M. Feliu, J. Kunze-Liebhäuser, Interfacial water structure as a descriptor for its electro-reduction on Ni(OH)₂-modified Cu(111), *ACS. Catal.* 11 (2021) 10324–10332, <https://doi.org/10.1021/acscatal.1c02673>.
- [33] K.-L.C. Nguyen, J.P. Bruce, A. Yoon, J.J. Navarro, F. Scholten, F. Landwehr, C. Rettenmaier, M. Heyde, B.R. Cuenya, The influence of mesoscopic surface structure on the electrocatalytic selectivity of CO₂ reduction with UHV-prepared Cu(111) single crystals, *ACS. Energy Lett.* 9 (2024) 644–652, <https://doi.org/10.1021/acsenergylett.3c02693>.
- [34] R.M. Arán-Ais, F. Scholten, S. Kunze, R. Rizo, B.Roldan Cuenya, The role of in situ generated morphological motifs and Cu(I) species in C₂⁺ product selectivity during CO₂ pulsed electroreduction, *Nat. Energy* 5 (2020) 317–325, <https://doi.org/10.1038/s41560-020-0594-9>.
- [35] N. Tian, Z.-Y. Zhou, S.-G. Sun, Y. Ding, Z.L. Wang, Synthesis of tetrahedral platinum nanocrystals with high-index facets and high electro-oxidation activity, *Science* (1979) 316 (2007), <https://doi.org/10.1126/science.1140484>, 732 LP–735.
- [36] N. Tian, Z.-Y. Zhou, N.-F. Yu, L.-Y. Wang, S.-G. Sun, Direct electrodeposition of tetrahedral Pd nanocrystals with high-index facets and high catalytic activity for ethanol electrooxidation, *J. Am. Chem. Soc.* 132 (2010) 7580–7581, <https://doi.org/10.1021/ja102177r>.
- [37] J. Xiao, S. Liu, N. Tian, Z.-Y. Zhou, H.-X. Liu, B.-B. Xu, S.-G. Sun, Synthesis of convex hexoctahedral Pt micro/nanocrystals with high-index facets and electrochemistry-mediated shape evolution, *J. Am. Chem. Soc.* 135 (2013) 18754–18757, <https://doi.org/10.1021/ja110583b>.
- [38] P. Sebastián, E. Vallés, E. Gómez, Copper electrodeposition in a deep eutectic solvent. First stages analysis considering Cu(I) stabilization in chloride media, *Electrochim. Acta* 123 (2014) 285–295, <https://doi.org/10.1016/j.electacta.2014.01.062>.
- [39] D.M. Kolb, M. Przasnyski, H. Gerischer, Underpotential deposition of metals and work function differences, *J. Electroanal. Chem. Interfacial. Electrochem.* 54 (1974) 25–38, [https://doi.org/10.1016/S0022-0728\(74\)80377-3](https://doi.org/10.1016/S0022-0728(74)80377-3).
- [40] A. Bagger, R.M. Arán-Ais, J. Halldin Stenlid, E. dos Santos, L. Arnarson, K. Degn Jensen, M. Escudero-Escribano, B. Roldan Cuenya, J. Rossmeisl, Ab initio cyclic voltammetry on Cu(111), Cu(100) and Cu(110) in acidic, neutral and alkaline solutions, *Chemphyschem.* 20 (2019) 1–11, <https://doi.org/10.1002/cphc.201900509>.
- [41] G.M. Brisard, E. Zenati, H.A. Gasteiger, N. Markovic, P.N. Ross, Underpotential deposition of lead on copper(111): a study using a single-crystal rotating ring disk electrode and ex situ low-energy electron diffraction and scanning tunneling microscopy, *Langmuir.* 11 (1995) 2221–2230, <https://doi.org/10.1021/la00006a060>.
- [42] J. Ustarroz, J.A. Hammons, T. Altantzis, A. Hubin, S. Bals, H. Terryn, A generalized electrochemical aggregative growth mechanism, *J. Am. Chem. Soc.* 135 (2013) 11550–11561, <https://doi.org/10.1021/ja402598k>.
- [43] P. Sebastián, E. Torralba, E. Vallés, A. Molina, E. Gómez, Advances in copper electrodeposition in chloride excess. A theoretical and experimental approach, *Electrochim. Acta* 164 (2015) 187–195, <https://doi.org/10.1016/j.electacta.2015.02.206>.
- [44] J. Li, X.-Y. Wang, X.-R. Liu, Z. Jin, D. Wang, L.-J. Wan, Facile growth of centimeter-sized single-crystal graphene on copper foil at atmospheric pressure, *J. Mater. Chem. C* 3 (2015) 3530–3535, <https://doi.org/10.1039/C5TC00235D>.
- [45] M. Liu, Y. Pang, B. Zhang, P. De Luna, O. Voznyy, J. Xu, X. Zheng, C.T. Dinh, F. Fan, C. Cao, F.P.G. de Arquer, T.S. Safaei, A. Mepham, A. Klinkova, E. Kumacheva, T. Filleter, D. Sinton, S.O. Kelley, E.H. Sargent, Enhanced electrocatalytic CO₂ reduction via field-induced reagent concentration, *Nature* 537 (2016) 382–386, <https://doi.org/10.1038/nature19060>.
- [46] L. Liang, Q. Feng, X. Wang, J. Hübner, U. Gernert, M. Heggen, L. Wu, T. Hellmann, J.P. Hofmann, P. Strasser, Electroreduction of CO₂ on Au(310)/Cu high-index facets, *Angewandte Chem. Int. Ed.* 62 (2023) e202218039, <https://doi.org/10.1002/anie.202218039>.
- [47] T.P. Moffat, Oxidative chloride adsorption and lead up on Cu(100): investigations into surfactant-assisted epitaxial growth, *J. Phys. Chem. B* 102 (1998) 10020–10026, <https://doi.org/10.1021/jp9828888>.
- [48] C. Xiao, N. Tian, W.-Z. Li, X.-M. Qu, J.-H. Du, B.-A. Lu, B.-B. Xu, Z.-Y. Zhou, S.-G. Sun, Shape transformations of Pt nanocrystals enclosed with high-index facets and low-index facets, *CrystEngComm.* 23 (2021) 6655–6660, <https://doi.org/10.1039/D1CE00949D>.
- [49] O.J. Wahab, M. Kang, E. Daviddi, M. Walker, P.R. Unwin, Screening surface structure–electrochemical activity relationships of copper electrodes under CO₂ electroreduction conditions, *ACS. Catal.* 12 (2022) 6578–6588, <https://doi.org/10.1021/acscatal.2c01650>.
- [50] J. Timoshenko, A. Bergmann, C. Rettenmaier, A. Herzog, R.M. Arán-Ais, H.S. Jeon, F.T. Haase, U. Hejral, P. Grosse, S. Kühn, E.M. Davis, J. Tian, O. Magnussen, B. Roldan Cuenya, Steering the structure and selectivity of CO₂ electroreduction catalysts by potential pulses, *Nat. Catal.* 5 (2022) 259–267, <https://doi.org/10.1038/s41929-022-00760-z>.
- [51] F. Scholten, K.-L.C. Nguyen, J.P. Bruce, M. Heyde, B.Roldán Cuenya, Identifying structure-selectivity correlations in the electrochemical reduction of CO₂: comparison of well-ordered atomically-clean and chemically-etched Cu single crystal surfaces, *Angewandte Chem.* 133 (2021) 19318–19324, <https://doi.org/10.1002/ange.202103102>.